END-OF LIFE DISPOSAL OF SPACECRAFT IN HIGHLY ELLIPTICAL ORBITS BY MEANS OF LUNI-SOLAR PERTURBATIONS AND MOON RESONANCES

Camilla Colombo[(1)], Elisa Maria Alessi[(2)], Markus Landgraf[(3)]

[(1)] University of Southampton, Highfield, SO17 1BJ Southampton, UK, Email: c.colombo@soton.ac.uk
[(2)] IFAC-CNR, Via Madonna del Piano 10, 50019 Sesto Fiorentino (FI), Italy, Email: em.alessi@ifac.cnr.it
[(3)] ESA/ESOC, Robert-Bosch-Straße 5, D-64293 Darmstadt, Germany, Email: Markus.Landgraf@esa.int

ABSTRACT

This paper presents a preliminary investigation of some possible strategies for the disposal of spacecraft on Highly Elliptical Orbits at the end-of-life. The effect of luni-solar perturbations is analysed through a simplified phase space model. This allows identifying the conditions for re-entry in the Earth's atmosphere. As a second strategy, Moon resonances are studied to increase the orbit perigee and transfer the spacecraft on weak capture orbits.

1 INTRODUCTION

In this work, we consider the exploitation of luni-solar perturbations for the disposal of Highly Elliptical Orbits (HEO) about the Earth. Such orbits are widely exploited because they are convenient not only for telecommunication purposes, but also for astrophysics missions, such as INTEGRAL, and XMM-Newton. Indeed, they guarantee spending most of the time at an altitude outside the Earth's radiation belt to avoid noise, and thus enabling long periods of uninterrupted scientific observation. Moreover, some HEO, such as Molniya and Tundra orbits, ensure a maximum time of flight in the coverage regions of the ground stations situated at the sub-apogee point, enhancing communication links. If the inclination is properly selected, HEO can minimise or nullify the duration of the spacecraft motion inside the eclipses. Because of their importance, it is crucial to clear these regions at the end-of-mission.

The dynamics of HEO with high apogee altitude is mainly influenced by the effect of third body perturbation due to the gravitational attraction of the Moon and the Sun. The variation of the orbit over time can be described through the variation of Keplerian elements double averaged over one orbit evolution of the s/c and over one orbital revolution of the perturbing body [1]. The luni-solar attraction induces long-term and secular variation in the eccentricity, inclination, argument of the node and argument of perigee.

In this paper two strategies are proposed to achieve the end-of-life disposal of HEO. A first strategy aims at lowering the perigee altitude so that the spacecraft can perform a controlled re-entry into the atmosphere. The natural libration in inclination and eccentricity (and thus perigee altitude) whose evolution depends on the value of the argument of the perigee with respect to the Earth-Moon plane is exploited [1]. Δv manoeuvres can be designed to enlarge the amplitude of the oscillation of eccentricity, so that the re-entry altitude can be reached.

The second strategy considers a weak capture trajectory at the Moon computed assuming the Circular Restricted Three-Body Problem (CR3BP) approximation [3]. Hyperbolic invariant manifolds associated with Libration Point Orbits (LPO) at the Lagrangian point either L_1 or L_2 can be used to design such an orbit. To target a lunar weak capture an increase of apogee altitude of the HEO and a decrease of its inclination are needed to exploit the lunar perturbation. This will allow raising the perigee altitude to the minimum distance the hyperbolic manifold can take with respect to the Earth. Deep or shallow resonances with the Moon mean motion are studied to achieve an increase of the perigee. A series of small Δv manoeuvres are allowed at the perigee to meet successive resonances.

In the design of the two strategies, the third body effect of the Moon is treated either in terms of long-term and secular variation of the orbital elements, or as CR3BP. While in the first case the orbital elements can be assumed constant over one revolution of the spacecraft, when capture trajectories are targeted, the semi-major axis is not constant anymore, on the other end it increases through Moon fly-bys. One approach or the other is selected based on the distance from the Moon.

A test case scenario is designed based on the orbit of the INTEGRAL mission that has currently been extended to 31 Dec. 2014. Based on the natural evolution of the orbit under perturbations, a preliminary analysis is performed to assess the required fuel consumption for the disposal manoeuvre at different times.

2 LUNI-SOLAR PERTURBATIONS

The dynamics of HEO with high apogee altitude is mainly influenced by the effect of third body

Proc. '6th European Conference on Space Debris'
Darmstadt, Germany, 22–25 April 2013 (ESA SP-723, August 2013)

perturbation due to the gravitational attraction of the Moon and the Sun and the effect of the Earth oblateness. Cook's formulation gives the secular and long-periodic perturbation due to luni-solar perturbation obtained through averaging over one orbit revolution of the satellite [4]. It assumes circular orbit for the disturbing bodies and considers only first terms of a/a_D, where a and a_D are respectively the spacecraft and the disturbing body semi-major axis [5]. However, they do take into account the obliquity of the Sun and the Moon over the equator and the precession of the Moon plane due to the Earth oblateness (in a period of 18.6 years with respect to the ecliptic). Alternatively, Chao gives another form of the averaged equations obtained from an expansion of the disturbing function from third-body perturbations [6]. The numerical propagation of the orbit of INTEGRAL considering secular and long term perturbations due to J_2 and luni-solar perturbations, from Oct. 2002 to January 2021, is compared against the actual ephemerides of INTEGRAL (from NASA Horizon) in Figure 1.

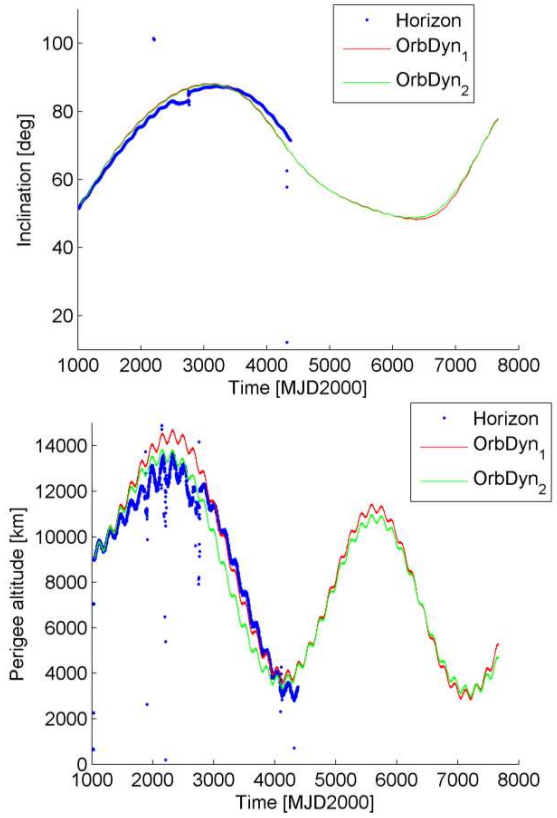

Figure 1. Orbit evolution of INTEGRAL between 2002 and 2021. Blue line: ephemerides (Horizon, NASA), red and green: numerical propagation with J_2 and luni-solar effect with Cook [1] and Chao's formulation [6].

Note that no manoeuvres have been applied in the simulation, whereas the actual evolution of INTEGRAL may contain some correction manoeuvres. The perigee altitude varies from over 13000 km in 2006 to a minimum of 2756 km on Oct. 2011. Also the inclination oscillates between a maximum of 87° to 48° [7].

Under the further assumption that the orbital elements do not change significantly during a full revolution of the perturbing body, the variation of the orbit over time can be approximately described through the variation of Keplerian elements double averaged over one orbit evolution of the s/c and over one orbital revolution of the perturbing body (either the Moon or the Sun) to give [1].

$$
\begin{aligned}
&\frac{d\bar{a}}{dt} = 0 \\
&\frac{d\bar{e}}{dt} = \frac{15}{8}\frac{\mu_D}{\mu_{\text{Earth}}} n \left(\frac{a}{r_D}\right)^3 e\sqrt{1-e^2}\sin^2 i \sin 2\omega \\
&\frac{d\bar{i}}{dt} = -\frac{15}{16}\frac{\mu_D}{\mu_{\text{Earth}}} n \left(\frac{a}{r_D}\right)^3 \frac{e}{\sqrt{1-e^2}}\sin 2i \sin 2\omega \\
&\frac{d\bar{\Omega}}{dt} = -\frac{3}{4}\frac{\mu_D}{\mu_{\text{Earth}}} n \left(\frac{a}{r_D}\right)^3 \frac{\cos i}{\sqrt{1-e^2}}\left(1-e^2+5e^2\sin^2\omega\right) \\
&\frac{d\bar{\omega}}{dt} = \frac{3}{4}\frac{\mu_D}{\mu_{\text{Earth}}} n \left(\frac{a}{r_D}\right)^3 \frac{1}{\sqrt{1-e^2}} \cdot \\
&\qquad \left(5\cos^2 i \sin^2\omega + \left(1-e^2\right)\left(2-5\sin^2\omega\right)\right) \\
&\frac{d\bar{h}_p}{dt} = -a\frac{d\bar{e}}{dt}
\end{aligned}
\tag{1}
$$

where a, e, i, Ω, ω, and h_p are respectively the osculating semi-major axis, eccentricity, inclination, argument of the ascending node, argument of the perigee, and perigee altitude measured in a reference system lying in the perturbing body-Earth plane, with the x-axis which follows the motion of the perturbing planet on this plane, μ_{Earth} is the gravitational constant of the Earth and μ_D is the gravitational constant of the disturbing body, either the Sun or the Moon and n the orbital speed $\sqrt{\mu_{\text{Earth}}/a^3}$. Note that the evolution of the argument of nodes is decoupled from the other orbital elements. The luni-solar attraction induces long-term and secular variation in the eccentricity, inclination, argument of the node and argument of perigee. From Eq. (1) it is clear that the both the inclination and the perigee altitude increase if $\pi/2 < \omega < \pi$ and $3/2\pi < \omega < 2\pi$ and they decrease if $0 < \omega < \pi/2$ and $\pi < \omega < 3/2\pi$. For a given value of i, the maximum change is for $\omega = \pi/4 + k\pi/2$ with k an integer number.

Considering an eccentricity in the interval $[0.79 \quad 0.88]$, which is the one INTEGRAL covers, ω decreases if i and ω belong to the intervals shown in Figure 2. In the case of INTEGRAL, from Jan. 2015 to about middle of Feb. 2019 ω is in the range

corresponding to the decrease of the inclination and the perigee altitude. During these years, ω will decrease until about Mar. 2017, and increase thereafter.

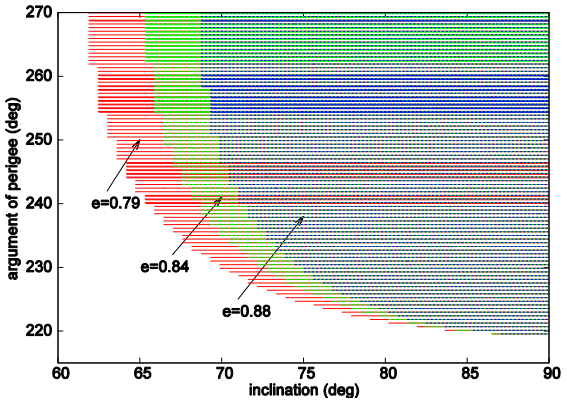

Figure 2. Range of inclination and argument of perigee (in the Earth-Moon orbital plane) for different values of the eccentricity, associated with a decrease of the argument of the perigee.

These and other considerations were, for example, taken into account for optimising the operational orbit of the INTEGRAL mission [8]. In a similar way luni-solar perturbations, coupled with the J_2 perturbation, may play a role in speeding the orbital decay of certain classes of HEO, by lowering the perigee altitude or in the other way around be exploited to increase the perigee altitude.

3 KOZAI ANALYTICAL THEORY FOR THIRD BODY PERTURBATION

The analytical theory on secular perturbations of orbits at high inclination and eccentricity by Kozai is here applied to analyse the secular evolution of an highly eccentric and inclined Earth centred orbit under the effect of the Moon perturbation [1]. The third body effect of the Sun and Earth oblateness are neglected. By developing the disturbing function in terms of $\alpha = a/a_D$, the ratio of the semi-major axis of the spacecraft and the Moon, and using Delaunay's transformations, the dynamics equations can be described through a time-independent Hamiltonian. The evolution of the orbit under lunar perturbation can be plotted on the $(2\omega, e)$ plane, where ω is the argument of perigee measured from the Earth-Moon plane. The initial condition of the spacecraft's orbit in terms of *a*, *e*, *i*, and ω, defines a contour line in the $(2\omega, e)$ plane, which represents the trajectory of the long term evolution of the spacecraft. Figure 3 represents the phase space trajectories for $\alpha = 0.23$, which correspond a semi-major axis of 87736.34 km and $a_D = 381400$ km the mean distance Earth-Moon. The black line approximates the trajectory of an INTEGRAL-like spacecraft with respect to the Earth-Moon plane by considering its ephemerides on 01/06/2013. Note that, in this simplified model, we assume the Moon to be at zero inclination with respect to the ecliptic plane. Future work will consider the actual inclination of the Moon with respect to the ecliptic. One equilibrium solution exists in correspondence of $\omega = \pi/2$ and for initial condition around the stationary point, such that in the case of INTEGRAL, the trajectory is librational. This means that the evolution of ω and eccentricity is bounded. The evolution of the inclination is determined by *e* and ω from $\Theta = (1-e^2)\cos^2 i$ which is a constant of the phase space (see Figure 4). As α increases or Θ decreases, the stationary solution moves to higher eccentricities. This can be seen in Figure 5 with red lines.

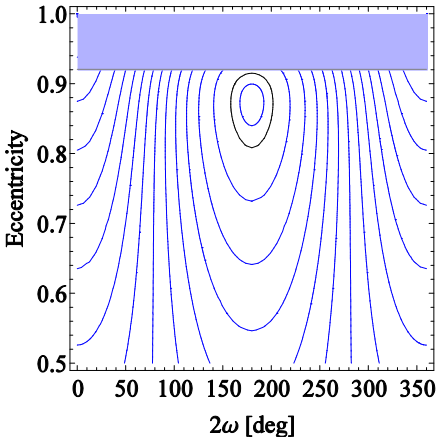

Figure 3 $(2\omega, e)$ phase space evolution under third-body perturbation. Black line: INTEGRAL-like s/c.

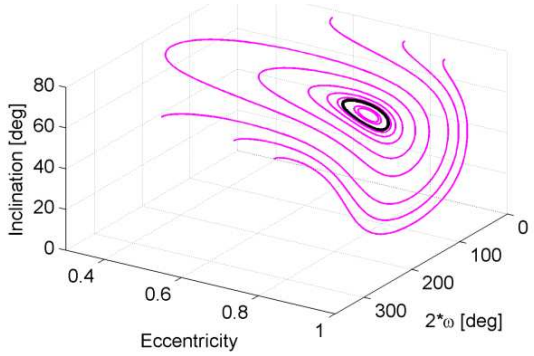

Figure 4. Evolution of the inclination as a function of e and 2ω.

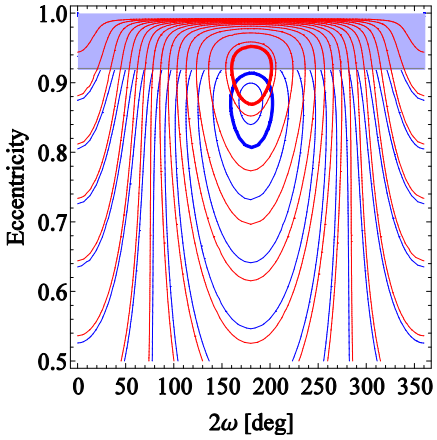

Figure 5. $(2\omega, e)$ *phase space evolution under third-body perturbation. Blue lines:* $\Theta = 0.03804$, *red lines:* $\Theta = 0.01513$ *which corresponds to an increase of eccentricity of 0.1 with respect to INTEGRAL's.*

4 STRATEGY FOR AN EARTH RE-ENTRY

The analysis of the $(2\omega, e)$ phase space can be exploited to analyse possible strategies for HEO spacecraft disposal at the end-of-life. The initial conditions of the spacecraft identify a trajectory in the phase space, hence is possible to design manoeuvres to move to another trajectory in the phase space. In case we want to target a re-entry, the spacecraft needs to transfer on a phase space trajectory that, at a certain time, reaches a critical eccentricity, in correspondence of which the perigee enters the Earth's atmosphere:

$$e_{\text{crit}} = 1 - \left(R_{\text{Earth}} + h_{p,\,\text{drag}}\right)/a \qquad (2)$$

A manoeuvre (or series of manoeuvres) which modifies only ω and e and i so that Θ remains constant allows transferring on a different line of the same phase space (for re-entry we would aim at a larger line). A manoeuvre (or series of manoeuvres) which changes only the semi-major axis would allow moving the stationary points, and hence the centre of libration of the phase space line. In order to assess the manoeuvre for re-entry in the phase space, we selected four initial conditions, positioned respectively at the minimum and maximum eccentricity and at the minimum and maximum 2ω. From each of these points, an optimisation procedure was used to determine the true anomaly for the manoeuvre along the orbit f and the Δv magnitude and direction $(\Delta v, \delta, \beta)$ such that, in the following evolution the condition $e(t^*) = e_{\text{crit}}$ is met

$$\min_{\{\Delta v, \delta, \beta, f\}} \Delta v \qquad C : \max\left[e(t)\right] = e_{\text{crit}}$$

Gauss planetary equations for finite differences where used to compute the change in orbital elements [9], then the following orbit evolution was computed through Eqs. (1). A multi-start method was initiated, followed by local constrained optimisation of the best solutions. Figure 6 shows the phase space trajectory obtained in each case and the corresponding manoeuvre: M_1 is the manoeuvre at the $\min e$ point (green), M_2 is the manoeuvre at the $\max e$ point (magenta), M_3 is the manoeuvre at the $\min(2\omega)$ point (red), and M_4 is the manoeuvre at the $\max(2\omega)$ point (cyan). It is interesting to note that in the four cases, although the manoeuvre is different, the spacecraft reaches the same phase space line.

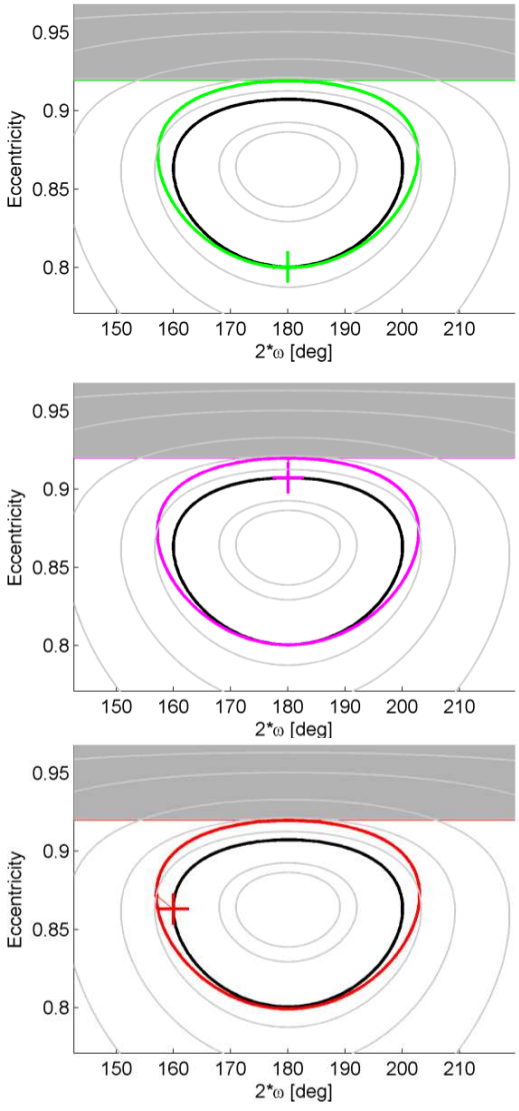

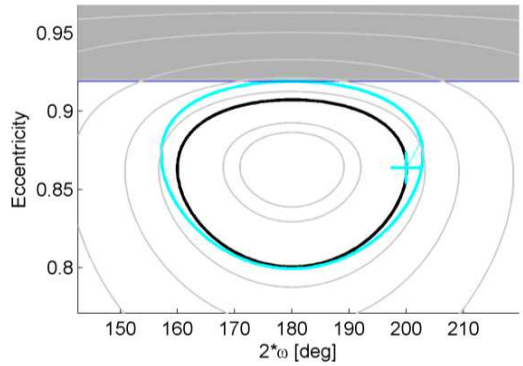

Figure 6. Phase space trajectory to decrease the perigee to 600 km. The cross indicates where the Δv manoeuvre is applied. From the top: M_1, M_2, M_3, M_4.

This can be also seen in the 3D representation in Figure 7 where the initial phase space trajectory is the black line and the phase space trajectory after the Δv manoeuvre is the magenta line. Note that in the case of $\min e$ the manoeuvre increases the inclination, hence decreases Θ, in the case of $\max e$ the manoeuvre increases the eccentricity hence again Θ is decreased. In both cases the semi-major axis is decreased, which also decreases the value of e_{crit} to be reached.

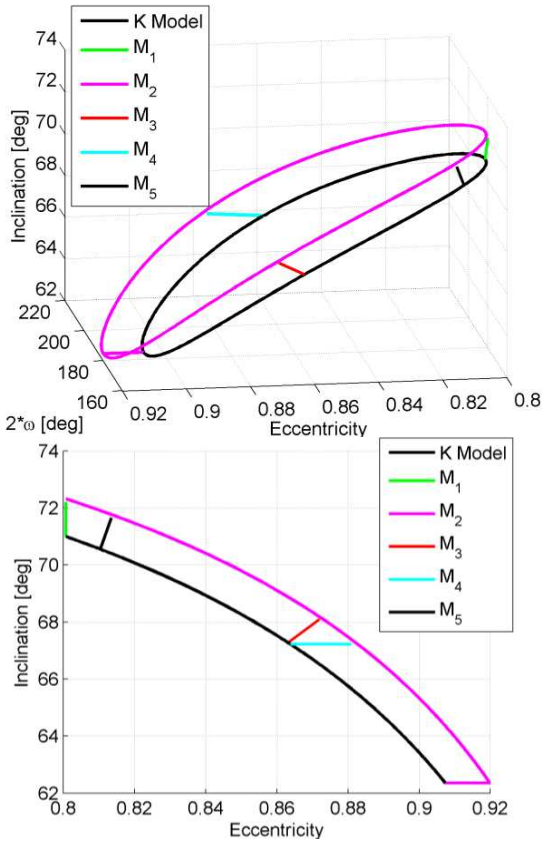

Figure 7. Phase space trajectory to decrease the perigee to 600 km.

Table 1: Δv requirements to for re-entry to 600 km.

Manoeuvre	**Value [km/s]**
M_1	0.04823
M_2	0.03185
M_3	0.03398
M_4	0.04506
M_5	0.04028

The cases of $\min e$ (green line) and $\max e$ (magenta line) and $\min(2\omega)$ (red line) were then solved also by considering the more accurate model of perturbations (luni-solar and J_2) and the result is shown in Figure 8 and Table 2. Note that, the Δv requirements in the full-dynamical case are not expected to be optimal as they were computed with local optimisation using as first guess the simplified model. Moreover, in the real scenario, J_2 and solar perturbation play an important role. A future work will include the J_2 effect and solar perturbation in a simplified phase space model.

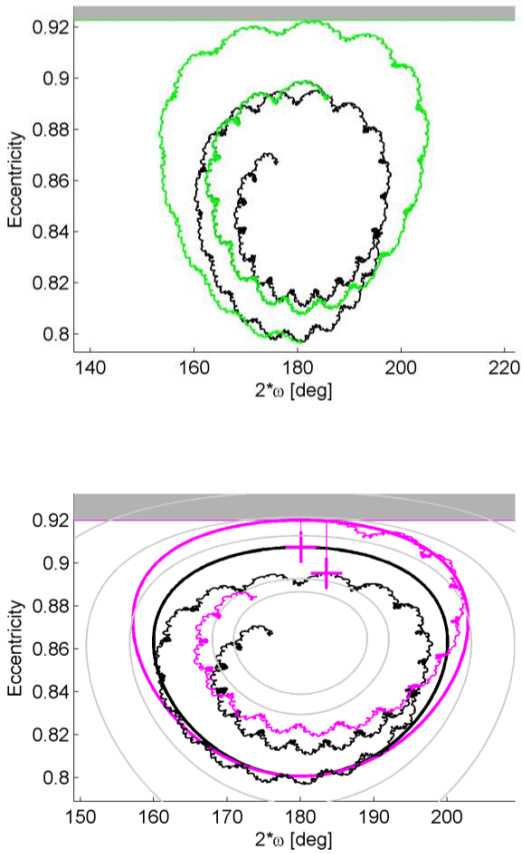

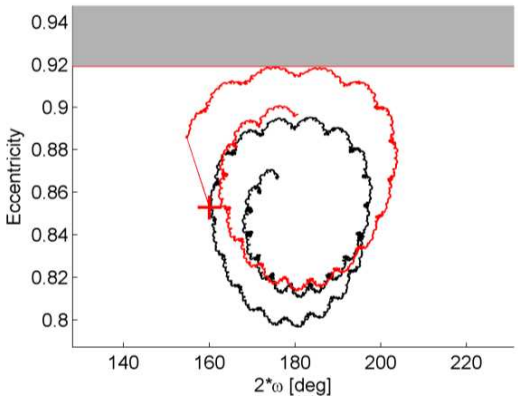

Figure 8. Phase space trajectory to decrease the perigee to 600 km with full dynamical model.

Table 2: Δv requirements to decrease the perigee to 600 km with full dynamical model.

Manoeuvre	**Value [km/s]**
$M_{1\ \text{full dynamical model}}$	0.10746
$M_{2\ \text{full dynamical model}}$	0.05811
$M_{3\ \text{full dynamical model}}$	0.08222

Note also that the manoeuvre M_2 correspond to a manoeuvre performed at the apogee of $-\Delta v_t$ in tangential direction to decrease the perigee of Δh_p. In this case, the required Δv can be simply computed as:

$$\Delta v_{t,\,\text{apo}} = \Delta h_p \sqrt{\mu_{\text{Earth}}} \Big/ 4a^{3/2} \sqrt{(1+e)/(1-e)} \qquad (3)$$

Figure 9 compares the results obtained in Table 2 to the Δv to decrease the perigee altitude of INTEGRAL below 600 km, applying a single manoeuvre at the apogee as in Eq. (3). The red line shows the remaining Δv capabilities assuming the spacecraft specific impulse of 235 s [10].

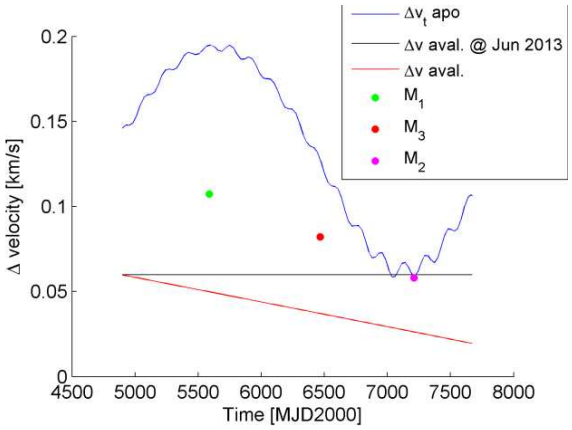

Figure 9. Δv requirements to decrease the perigee with a single manoeuvre at the apogee.

5 WEAK CAPTURE TRAJECTORIES

The second disposal strategy considered here aims at transferring the s/c on a weak capture orbit at the Moon. This can be designed by considering that at the same time Earth and Moon affect the motion of the spacecraft. In this way, the probe can be captured inside the gravitational sphere of influence of the Moon for a sufficiently high amount of time, without being inserted into an orbit about it. In principle, no propellant would be required to orbit around the Moon and then move away from it, as there exist trajectories that naturally achieve this purpose. The methodology implemented here is established on the unstable invariant manifold which arises in the neighbourhood of the collinear equilibrium point L_1 in the CR3BP approximation [11],[12],[13]. Other strategies, such as an analysis of the orbital elements with respect to the Moon based on the double averaged equations or the exploitation of heteroclinic connections between L_1 and L_2 hyperbolic manifolds, can be found for instance in [14]. We recall that in the CR3BP model, the spacecraft is assumed massless and affected only by the gravitational attraction of Earth and Moon, which move on circular orbits around their common centre of mass [3]. The canonical synodical reference system and the set of non-dimensional units such that μ=0.01215 is the mass parameter, the unit of length is equal to 384400 km and the unit of velocity is 1.0231 km/s. It is well-known that this dynamical model admits five equilibrium points, L_1-L_5 and that there exists one first integral of motion, representing the energy of the probe, namely C_J. Depending on the value of C_J there might exist regions where the motion is forbidden. In the neighbourhood of each collinear equilibrium point (L_1, L_2, L_3) there exist a central and a hyperbolic invariant manifold [11],[12],[13]. The central manifold is filled with periodic (e.g., Lyapunov and halo) and quasi-periodic (e.g., Lissajous and quasi-halo) orbits (plus some chaotic regions), and to each of such bounded solutions correspond one stable and one unstable invariant manifold. They look like tubes of asymptotic trajectories tending to, or departing from, the corresponding orbit. When going forward in time, the trajectories on the stable manifold approach exponentially the periodic/quasi-periodic orbit, while those on the unstable manifold depart exponentially from it. The boundary between the Earth and the Moon realms is represented by the Hill's sphere, whose radius is defined as $R_{\text{Hill}} = (\mu/3)^{1/3} \sim 61273$ km. To design a gravitational capture we propagate forward in time for about 270 days the unstable invariant manifold associated with halo and vertical Lyapunov periodic L_1 orbits until the corresponding trajectories escape either from the Moon's realm or impact onto the Moon. A disposal towards these paths can be convenient to extend the mission lifetime, to perform some

observations of the lunar environment, provided that they can orbit the Moon down to about 500 km. An example is shown in Figure 10.

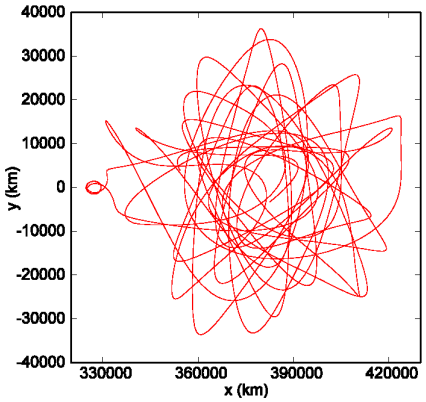

Figure 10. Example of weak capture trajectory at the Moon. x-y projection in the synodical reference system, where the Moon is located at (379729.32, 0) km.

In order to exploit the dynamics corresponding to the hyperbolic manifolds, the initial orbit at the Earth must fulfil three conditions: $h_p \in [90000 \quad 150000]$ km, $h_a \sim$ 300000 km and the hyperbolic excess velocity computed at the boundary of the Hill's sphere, that is, at the encounter with the Moon, must be lower than 0.5 km/s. In this work, we assume that it is possible to raise the apogee of the orbit at the desired altitude, with impulsive manoeuvres and by exploiting luni-solar perturbations as shown in Section 3. It has been computed that using a single manoeuvre at the perigee with the available propellant in June 2013, it is possible to increase INTEGRAL apogee to 207901 km, hence natural perturbations should be also exploited. The other two requirements can be met by implementing a so-called endgame [15]. The endgame strategy has been studied and adopted recently by several authors, for the Earth - Moon system in particular in [16],[17]. By taking advantage of successive perturbations of the Moon on the probe, the energy and thus the semi-major axis associated with the initial orbit can be changed. If we further consider putting the s/c in mean motion resonance with the Moon, this effect can be enhanced. We recall that two bodies are in mean motion resonance if their periods satisfy an l/m ratio with $m, l \in \mathbb{N}$. In this case, they encounter after l revolutions of the first body (i.e., Moon) and m revolutions of the second one (i.e., s/c). Here we use only l:m resonances, where $l < m$, as the probe is expected to move in between Earth and Moon.

The perturbation of the Moon takes place at the apogee: according to the angle of approach it increases or decreases the perigee and thus the semi-major axis corresponding to the osculating ellipse of the probe around Earth. After the encounter, the period of the orbit changes and another type of resonance has to be considered. It is possible to move from one resonance to the other either ballistically or with a small manoeuvre whose direct consequence is to change the altitude of the apogee. The most favourable angle of approach can be targeted by tuning conveniently the resonance chosen, that is, it can be deep or shallow. Figure 11 shows an example of endgame to target a weak capture trajectory computed starting from a vertical Lyapunov L_1 orbit. In this case three manoeuvres are applied to jump on a 1:2, 1:3, 1:3 resonance sequence backward in time for a total Δv of 0.074 km/s. From the perigee of the unstable manifold to the minimum perigee achieved, which is about 18064 km, it takes 80 days.

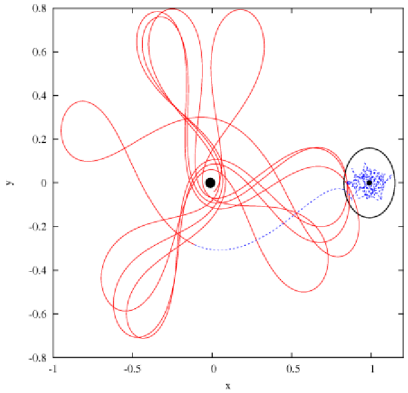

Figure 11. x-y projection of a weak capture trajectory (blue) at the Moon obtained by propagating the unstable invariant manifold of a vertical Lyapunov L_1 orbit and endgame strategy (red). Synodical reference system with non-dimensional units. The black circle represents the Hill's sphere at the Moon.

In Figure 12 and Figure 13 we show an example of endgame to target a weak capture trajectory computed starting from a halo L_1 orbit. In this case two manoeuvres are applied to jump on a 1:2, 1:3 resonance sequence backward in time for a total Δv of 0.062 km/s. After that, the trajectory evolves ballistically down to a perigee of about 17552 km in about 2.5 years.

This preliminary analysis demonstrates that a wide range of weak capture trajectories are possible and that the cost to get to the perigee of an INTEGRAL-type orbit is feasible (as a measure of comparison the remaining available Δv on board on 01/06/2013 has been estimated around 0.05980 km/s). A procedure to optimise the sequence of resonances is currently under study. The main drawback of this disposal strategy is, however, the inclination with respect to the Earth-Moon plane characterising the final orbit (in the backward propagation), which is never greater than 30º, much lower than the one associated with INTEGRAL and XMM-Newton. The exploitation of luni-solar

perturbations and the Earth oblateness to this aim and to increase the orbit apogee will be investigated.

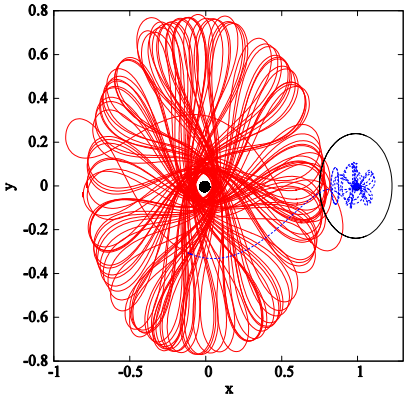

Figure 12. x-y projection of a weak capture trajectory (blue) at the Moon obtained by propagating the unstable invariant manifold of a halo L_1 orbit and endgame strategy (red). Synodical reference system with non-dimensional units. The black circle represents the Hill's sphere at the Moon.

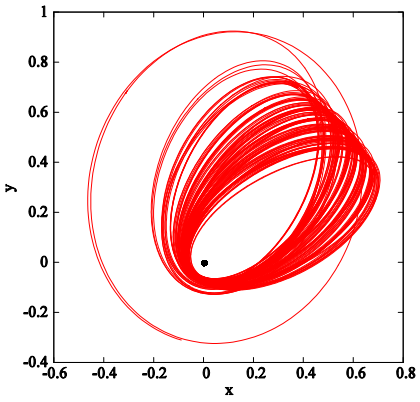

Figure 13. x-y projection of the endgame strategy of Figure 12 displayed in the inertial reference system centred at the Earth. Non-dimensional units.

6 CONCLUSIONS

This article presents a preliminary analysis of possible strategies for the disposal of Highly Elliptical Orbits. A phase space analysis of luni-solar perturbation allows designing manoeuvres for Earth re-entry, while Moon resonances can be exploited for injection in weak capture orbits with the Moon. Future work will deal with the optimisation of re-entry manoeuvres considering the full dynamical model and including multiple Δv manoeuvres. Moreover, the phase-space will be extended for designing stable orbits targeting.

7 ACKNOLEDGEMENTS

This work was performed as part of the ESA/GPS contract number ESA/ GSP-SOW-12-602. The authors would like to thank Dr. Alessandro Rossi for his valuable advices.

8 REFERENCES

[1] El'yasberg P. E. (1967). *Introduction to the theory of flight of artificial Earth satellites,* (translated from Russian) NASA, pp. 300-314.

[2] Kozai Y. (Nov. 1962). Secular Perturbations of Asteroids with High Inclination and Eccentricity. *The Astronomical Journal*, **67**(9), 591-598.

[3] Szebehely V. (1967). *Theory of orbits*, Academic Press, New York.

[4] Cook G. E., Luni-solar perturbations of the orbit of an Earth satellite. *Geophysiscal J.* **6**(271), 1962.

[5] Blitzer L. (1970). *Handbook of Orbital Perturbations*, Astronautics 453, Univ. of Arizona.

[6] Chao-Chun G. C. (2005). *Applied Orbit Perturbation and Maintenance*, AIAA, El Segundo, California, pp. 23-29.

[7] Hübner J. M., Southworth R. T., McDonald A., Kretschmar P., Lozano C., Walker M. INTEGRAL Revisits Earth - Low Perigee Effects on Spacecraft Components.

[8] Eismont N. A., Ditrikh A. V., Janin G., Karrask V. K., Clausen K., Medvedchikov A. I., Kulik S. V., Vtorushin N. A., Yakushin N. I., (Nov. 2003) Orbit design for launching INTEGRAL on the Proton/Block-DM launcher. *A. and A.*, **411**(1), L37–L41, doi: 10.1051/0004-6361:20031452

[9] Colombo C. (2010). *Optimal Trajectory Design for Interception and Deflection of near Earth Objects.* PhD thesis, University of Glasgow, Glasgow.

[10] Kessler M., "XMM-Newton Confirmation and Extension," 13 September 2010. [Online]. ftp://ftp.sciops.esa.int/pub/mkessler/XMM-Newton.pdf. [Accessed 04 Apr. 2013]

[11] Gómez G., Llibre J., Martínez R., Simó C. (2000). *Dynamics and Mission Design Near Libration Point Orbits - Volume 1: Fundamentals: The Case of Collinear Libration Points*, World Scientific, Singapore.

[12] Gómez G., Jorba À., Masdemont, Simó C. (2000). *Dynamics and Mission Design Near Libration Point Orbits -- Volume 3: Advanced Methods for Collinear Points*, World Scientific, Singapore.

[13] Koon W.S., Lo M.W., Marsden J.E., Ross S.D. (2008). *Dynamical Systems, the Three-Body Problem and Space Mission Design*, Marsden Books, ISBN 978-0-615-24095-4.

[14] Alessi E.M., Pergola P. (2012). Two options for

the Callisto's exploration, *Acta Astronaut.* 72, pp. 185-197.

[15] Johannesen J.R., D'Amario L.A. (1999). Europa Orbiter Mission Trajectory Design, *Adv. Astron.* Sci. 103, 895-908.

[16] Schoenmakers J., Pulido J., Cano J.L. (1999). SMART-1 Moon mission: Trajectory design using the moon gravity, ESA - Issue 1.

[17] Schoenmakers J. (2007). Cross-Scale Mission Analysis. Transfers using Moon Resonances, MAS Working Paper No. 511, ESA - Issue 1.